SIMULATION OF SEMICONDUCTOR DEVICES AND PROCESSES Vol. 4
Edited by W. Fichtner, D. Aemmer - Zurich (Switzerland) September 12-14, 1991 - Hartung-Gorre

Monte Carlo modeling encompassing the effective bulk state as well as quasi two-dimensional state of electrons in the MOS inversion layer

Syunji Imanaga, and Yoshinori Hayafuji
SONY Corporation Research Center, 174 Fujitsuka-cho, Hodogayaku, Yokohama, 240, Japan

Abstract

Electron transport in the Si MOS inversion layer was investigated by Monte carlo particle simulation. A new model is proposed, in which electrons in the MOS inversion layer were treated in one of two ways depending on the their energy: electrons with energy less than the threshold energy, E_{th}, were treated as being two dimensional, while electrons with energy larger than E_{th} were treated as being in bulk Si. the simulated results of the dependence of the drift velocity on the tangential electric field and the electric field normal to the MOS inversion layer are both in good agreement with the experimental results.

Several authors[1][2][3] have reported a microscopic model in which electrons in the MOS inversion layer are treated as quasi two-dimensional electron gas. Transport characteristics were obtained using the Monte Carlo method, but the calculated results and the experimental results are not in good agreement.

We have the following three questions about this type of simulation. (1) Are the transport characteristics of the hot electrons in the MOS inversion layer accurately obtained by taking account of only the 3 to 5 lowest subbands at room temperature ? (2) If only the 3 to 5 lowest subbands are taken into account, the scattering rate of quasi two-dimensional electrons with high energy is independent of electron energy. In such a situation, does not the electron energy continue to increase indefinitely ? (3) When the phonon types included in the simulation and the parameters of the phonon scattering rate of quasi two-dimensional electrons in the MOS inversion layer are the same as those in bulk Si, are valid simulation results of the transport characteristics of two-dimensional (2D) electrons obtained ?

The purpose of the present work is to answer these questions and to propose a microscopic model which gives simulation results in good agreement with Cooper and Nelson's[4] experimental results on the drift velocity.

1 Simulation Model

We consider the p-Si/SiO_2 inteface to be parallel to a [100] plane and the $\langle 011 \rangle$ direction of the n-inversion channel to be the direction of the driving field, in accordance with the configuration of Cooper and Nelson's experiments.

Bulk Si has six equivalent ellipsoidal valleys in the conduction band and a 2D electron system in a [100] plane (xy-plane) has one degenerate circular valley and four elliptic valleys. The relation between the valleys in bulk and 2D electron systems is shown in Figure 1.

Two types of subband series arise from the two equivalent valleys showing the longitudinal mass, m_l, in the direction of perpendicular to the [100] interface (z-direction) and the four equivalent valleys showing the transverse mass, m_t, in the same direction, which are denoted by E_0, E_1, E_2, ... and ...E_0', E_1', E_2'... respectively, using Stern and Howard's notation[5]. In the present simulation, the lowest three subbands were taken into account. Two models were investigated.

(1) Model 1 : pure 2D electron gas model

Electrons in the MOS inversion layer were treated as being two dimensional, taking account of the three lowest subbands. The subband structure was obtained by the method proposed by Stern[5], in which Schrödinger and Poisson equations are self-consistently solved. These equations are written as

$$\frac{d^2\psi_i}{dz^2} + \frac{2m}{\hbar^2}[E_i + e\phi(z)]\psi_i \;=\; 0 \tag{1}$$

and

$$\frac{d^2\phi(z)}{dz^2} \;=\; -[\rho_{depl} - e\sum_i N_i \mid \psi_i \mid^2]/\epsilon, \tag{2}$$

where ρ_{depl} is the depletion layer charge and N_i represents the number of electrons in subband i and is given in equilibrium by

$$N_i \;=\; \frac{n_v m_d k_B T}{\pi\hbar^2}\ln[1 + \exp(\frac{E_f - E_i}{k_B T})], \tag{3}$$

where n_v is valley degeneracy, m_d is the density of state effective mass and E_f is the Fermi energy. The subband denoted by E_i has n_v of 2 and m_d of m_t, and the subband denoted by E_i' has n_v of 4 and m_d of $(m_l m_t)^{1/2}$. Using these subband structures, we can perform Monte Carlo simulation of 2D electron gas in the inversion layer.

As scattering mechanisms of 2D electrons in the MOS inversion layer, we take account of the intra and inter subband scattering for coupled inter-valley phonons, intra and inter subband acoustic phonon scattering, screened fixed-charge scattering which includes both trapped interface charges and ionized impurities, and surface roughness scattering. We used the same phonon energies and the same coupling constants in the inter-subband scattering as those in intervalley scattering in bulk Si[6]. We used Price's formulation[7] for the inter-subband scattering rate and the acoustic phonon scattering rate. These are written by

$$P_{sb} \;=\; \frac{m_d D_0^2}{\hbar^2\rho\omega_0}\int \mid \psi_m(z) \mid^2 \mid \psi_n(z) \mid^2 dz \begin{bmatrix} N_i u_0(E - E' + \hbar\omega_0) \\ (N_i + 1)u_0(E - E' - \hbar\omega_0) \end{bmatrix} \tag{4}$$

and

$$P_{ac} \;=\; \frac{m_d D_{ac}^2 k_B T}{\hbar^3 \rho s_l^2}\int \mid \psi_m(z) \mid^2 \mid \psi_n(z) \mid^2 dz, \tag{5}$$

where D_0 and D_{ac} are the coupling constants independent of m and n; m_d is the density of state effective mass which is m_t for E_0 and E_1 subbands and $(m_l m_t)^{1/2}$ for the E_0' subband; $\hbar\omega_0$ is the phonon energy coupled with this transition; ρ is the mass density; E and E' are initial and final electron energy, respectively; u_0 is the unit step function; s_l is the sound velocity; and T is the lattice temperature. Table 1 shows the phonon type and valley degeneracy of the final state as related to inter-subband scattering as well as the initial and the final subbands

of the transition. For the trapped interface-charge and ionized-impurity scattering rates for 2D electrons, we used Ning and Sah's formula[8] including the screening effect, which is given by

$$P_{ion} = \frac{1}{2\pi\tau_0(E)}\int_0^{2\pi}(1+\frac{s}{q})^{-2}d\theta, \tag{6}$$

$$\frac{1}{\tau_0(E)} = \frac{\pi^2 e^4 N_I}{\hbar\bar{\epsilon}^2 E} \tag{7}$$

where N_I is the number of interface charges per unit area; $\bar{\epsilon} = (\epsilon_{oxide} + \epsilon_{Si})/2$ is the effective dielectric constant at the interface; E is the kinetic energy of the electron; $s = 2\pi e^2 N_s/(\epsilon_{Si} k_B T)$ is the screening parameter where N_s is the sheet carrier density; and $q = 2k\sin\theta$ where θ is the angle between initial wave vector k and final wave vector k'. The surface roughness scattering rate is given by[9]

$$P_{surf} = \frac{\pi m_d (\Delta\Lambda e E_{eff})^2}{\hbar^3}, \tag{8}$$

$$E_{eff} = \frac{e(N_s/2 + N_{depl})}{\epsilon_{Si}} \tag{9}$$

where Δ is the root mean square deviation of the surface from flatness; and Λ is the correlation length of roughness. The parameter of the product $\Delta \cdot \Lambda$ used in the present simulation is $1.0 \times 10^{-14} cm^2$ which fits the experimental results.

Figure 2(a) and (b) show the dependence of the total scattering rate on the electron kinetic energy of each subband for a low sheet carrier density of $N_s = 4.5 \times 10^{11} cm^{-2}$ and for a high sheet carrier density of $N_s = 3.8 \times 10^{12} cm^{-2}$, respectively. The scattering rate in the case of high sheet carrier density is larger than that in the case of low sheet carrier density except in the very low energy region.

(2) Model 2: 2D+bulk electron model

In Model 2, we use our value for threshold energy, E_{th}. E_{th} should be determined such that the subband wave functions with energy higher than E_{th} spread sufficiently to be able to ignore the electron confinement effect. An electron with energy lower than E_{th} is treated as two dimensional, while an electron with energy higher than E_{th} is treated as being in the bulk Si. Namely, 2D electrons with a total energy higher than E_{th} are transformed to the bulk electron state and electrons in the bulk state with a total energy lower than E_{th} are transformed back to the 2D electron state. The energy conservation and the conservation of momentum component parallel to the interface are taken into account in this transformation. The scattering mechanisms[10] included in the Monte Carlo simulation of the bulk Si are intervalley scattering, acoustic phonon scattering and ionized impurity scattering. Three g-phonons and three f-phonons are taken into account in the intervalley scattering. The parameters used in the present Monte Carlo simulation of bulk Si are the same as those of Jacoboni[6] except nonparabolicity parameter α of 0.35 eV^{-1} which is chosen to fit Jacoboni's experimental result. Figure 3 compares the experimental results of the dependence of bulk drift velocity on the electric field and the present best-fitted simulation results.

2 Simulation results and discussion

(a)Simulation using Model 1

We take the following equation, used by Cooper and Nelson, as an expression of the normal electric field E_n :

$$E_n = \frac{q[N_s/2 + N_{depl}]}{\varepsilon_{Si}}. \tag{10}$$

In the cases of $E_n = 4.0 \times 10^4, 9.0 \times 10^4, 1.3 \times 10^5$, and 3.0×10^5 V/cm, the inversion layer potentials, the subband energies, and the wave functions of the subbands are self-consistently calculated. The calculated results of the inversion layer potentials, the subband energies and the squares of the absolute values of subband wave functions are shown in Figure 4. In these figures, we can see that electrons in the inversion layer are more strongly confined as E_n increases.

Figure 5(a) shows a comparison between the drift velocities estimated from Cooper and Nelson's experimental formula and the present simulation results based on Model 1. In the low tangential electric field region, the drift velocity decreases as the normal electric field increases. We can see this same tendency in the experimental results. However, in a tangential electric field region higher than 10^4 V/cm, the simulated drift velocity decreases as the tangential electric field (E_t) increases, while the drift velocity derived from the experiment increases and then saturates as the tangential electric field increases. The simulated results disagree with the experimental results on this point. The decrease of the simulated drift velocity in a high tangential electric field becomes larger as the normal electric field decreases, that is, the confinement of electrons in the inversion layer weakens.

The drift velocity decrease in the high electric field region shown in Figure 5(a) can be attributed to the increase of the conduction effective mass which is caused by the nonparabolicity of the conduction valley and the enormously increased electron energy which is about 10 eV at the E_t of 10^5 V/cm. Figure 6 shows the dependence of the averaged electron kinetic energy on the tangential electric field with the normal electric field as a parameter calculated based on Model 1. Equation 11 shows the relation among drift velocity, nonparabolicity and electron energy:

$$V_d = \frac{\hbar k}{m^*(1 + 2\alpha E)}. \tag{11}$$

The reason why electron energy increases enormously is because the scattering rate of 2D electrons is independent of their energy in the high energy region. We found that Model 1 is not an accurate model of hot electron transport characteristics, so we propose Model 2.

(b) Simulation using Model 2

Figure 5(b) compares the dependence of the drift velocity on the tangential electric field using the drift velocities estimated from Cooper and Nelson's experimental formula and the simulation results derived from Model 2. As can be seen, the simulated v_d versus E_t curves are in good agreement with those estimated from Cooper and Nelson's experimental formula.

Figure 7 compares the dependence of the drift velocity on the normal electric field with the tangential electric field as a parameter, using Cooper and Nelson's experimental results and the present simulation using Model 2. As can be seen, the present simulation results based on Model 2 are in good agreement with the experimental results. The dependence of the averaged electron energy on the tangential electric field with E_n of 1.3×10^5 V/cm was simulated, based on Model 2. The energy value at the tangential electric field of 10^5 V/cm is 0.57 eV, which is much less than the simulated value derived using Model 1. This value seems of a reasonable order.

3 Conclusion

Monte Carlo simulations based on two models were carried out in order to obtain transport characteristics of electrons in the MOS inversion layer. Model 1 is a pure two-dimensional model taking account of the three lowest subbands. The simulation results based on Model 1 disagrees with the experimental results in the high electric field region. Model 2 encompasses the effective bulk state as well as quasi two-dimensional state of electrons in the MOS inversion layer. The simulated V_d versus E_t curves and V_d versus E_n curves based on Model 2 are both in good agreement with the experimental results of Cooper and Nelson.

It is important that the model encompasses the effective bulk electron state as well as the two-dimensional electron state in the simulation of the electron transport characteristics in MOS inversion layer.

References

[1] P. K. Basu, J. Appl. Phys. 48(1), 350(1977).

[2] C. Hao, J. Zimmermann, M. Charef, R. Fauquembergue and E. Constant, Solid State Electron. 28(8), 733(1985).

[3] K. Terashima, C. Hamaguchi and T. Taniguchi, Superlattices and Microelectronics 1(1), 15(1985).

[4] J. A. Cooper, Jr. and D. F. Nelson, J. Appl. Phys. 54(3), 1445(1983).

[5] F. Stern and W. E. Haward, Phys. Rev. 163(3), 816(1967).

[6] C. Jacoboni, R. Minder and G.Majni, J. Phys. Chem. Solids, 36, 1129(1975).

[7] P. J. price, Ann. Phys. 133, 217(1981).

[8] T. H. Ning and C. T. Sah, Phys. Rev. B6(12), 4605(1972).

[9] D. K. Ferry, Thin Solid Film 56, 243(1979).

[10] C. Jacoboni and L. Reggiani, Rev. Mod. Phys. 55(3), 645(1983).

Table 1: Related phonon types in the subband transition. Valley degeneracy of the final state is given in the parenthesis.

Initial subband	*Final subband*		
	E_0	E_1	E_0'
E_0	3 g-phonon(1) acoustic phonon(1)	3 g-phonon(1) acoustic phonon(1)	3 f-phonon(4)
E_1	3 g-phonon(1) acoustic phonon(1)	3 g-phonon(1) acoustic phonon(1)	3 f-phonon(4)
E_0'	3 f-phonon(2)	3 f-phonon(2)	3 g-phonon(1) 3 f-phonon(2) acoustic phonon(1)

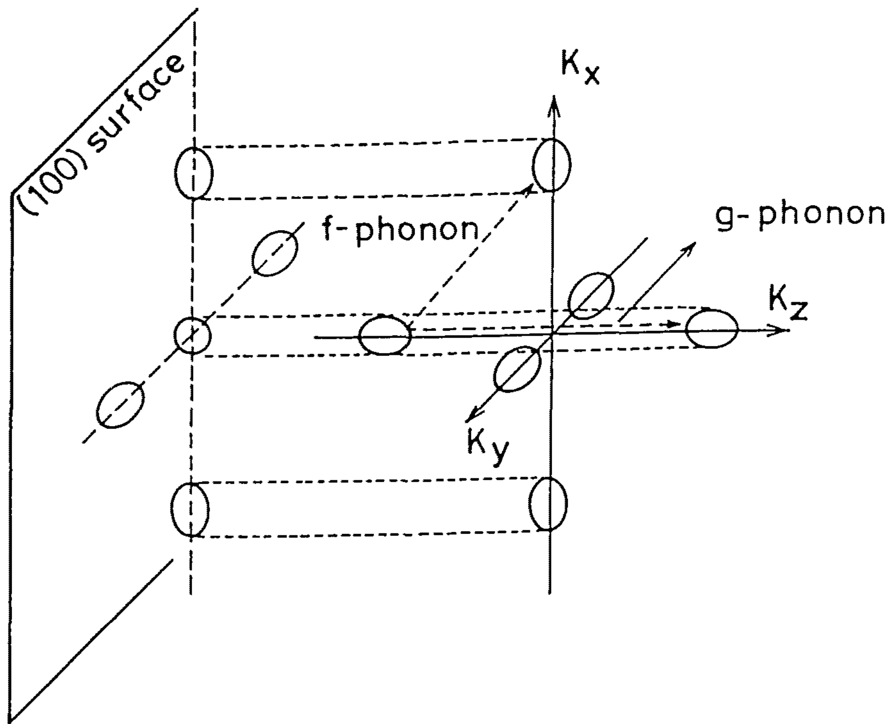

Figure 1: Schematic representation of the constant energy surfaces of bulk Si and two-dimensional electron gas for the [100] Si plane.

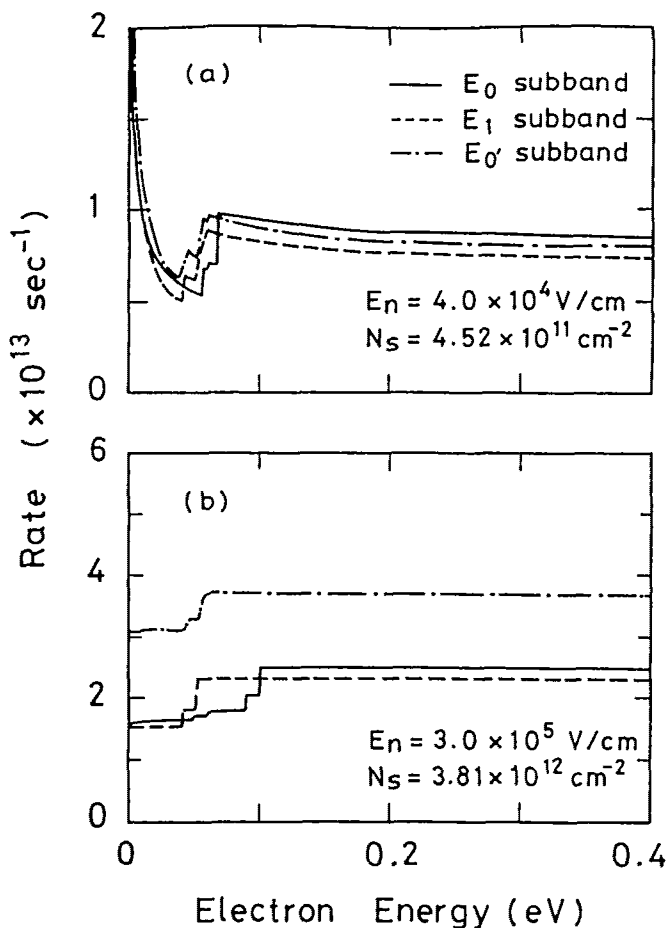

Figure 2: Total scattering rate versus kinetic energy of two-dimensional electron of E_0, E_1, and E'_0 subband for (a) low sheet carrier density of $N_s = 4.5 \times 10^{11} cm^{-2}$ and (b) high sheet carrier density of $N_s = 3.81 \times 10^{12} cm^{-2}$.

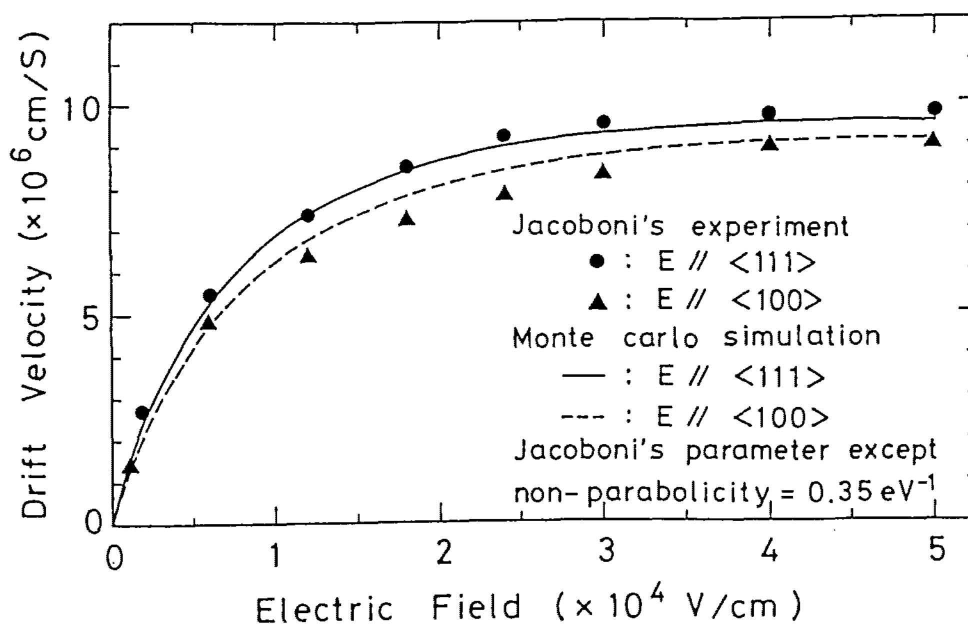

Figure 3: Electron drift velocity in bulk Si as a function of electric field. Closed circles and closed triangles refer to experimental data[6] with the electric field parallel to ⟨111⟩ and ⟨100⟩ direction, respectively. The continuous and broken lines indicate the best fitted present simulation results with the electric field parallel to ⟨111⟩ and ⟨100⟩ direction, respectively.

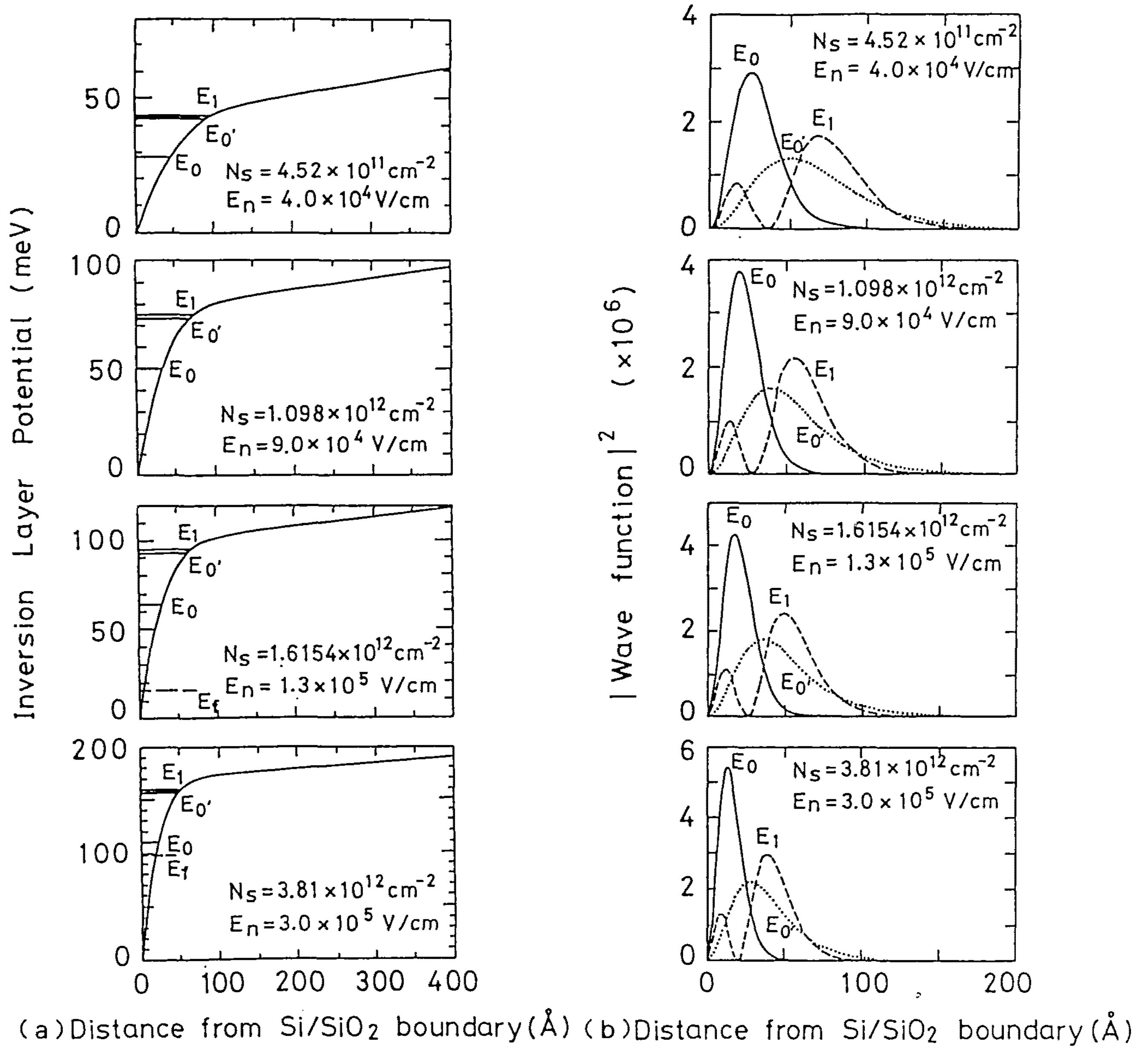

Figure 4: Self-consistently calculated (a) potentials and subband energies, and (b) squares of subband wave functions of two-dimensional electron in MOS inversion layer for the normal electric fields of $4.0 \times 10^4, 9.0 \times 10^4, 1.3 \times 10^5$ and 3.0×10^5 V/cm, respectively.

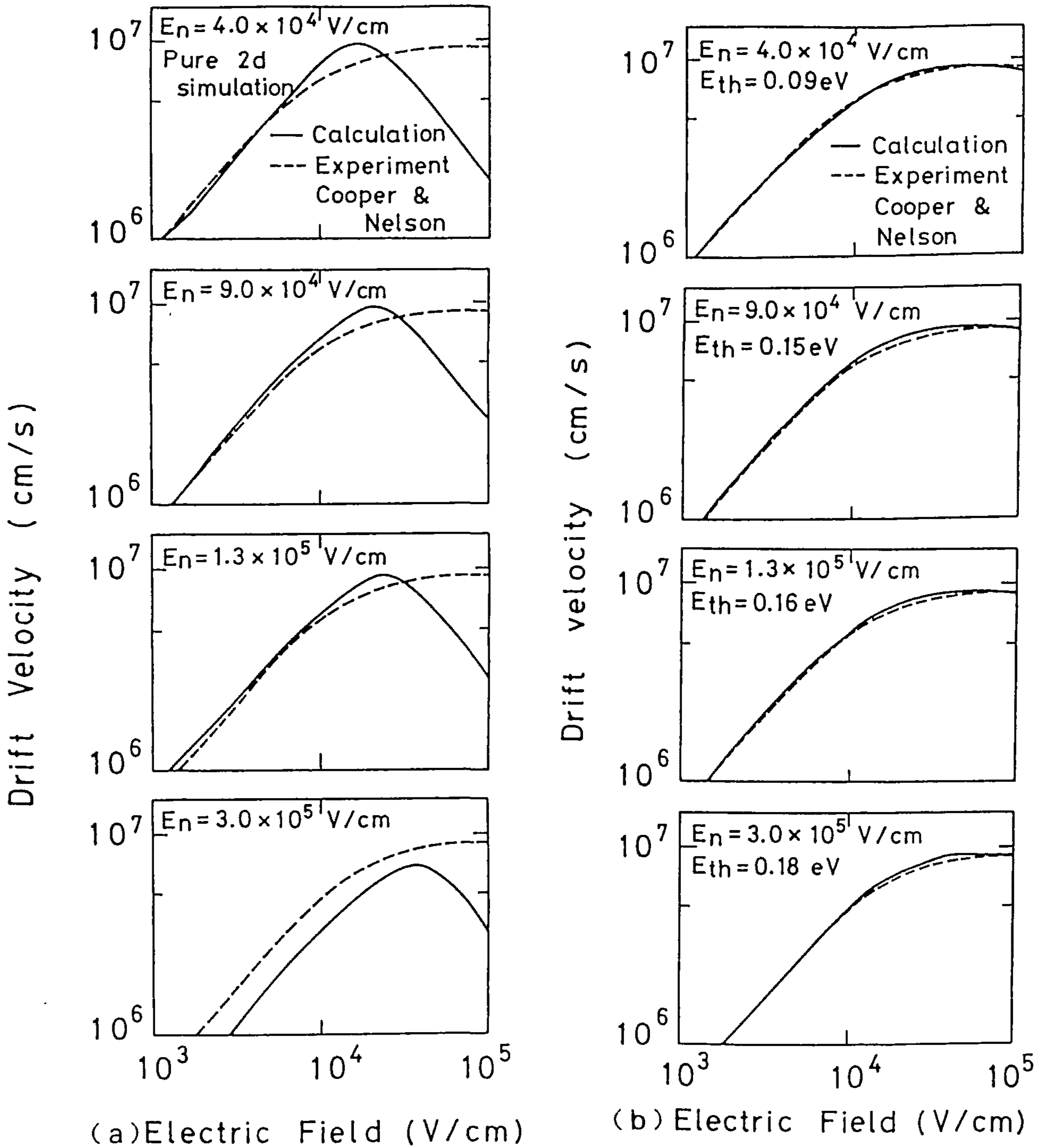

Figure 5: Drift velocity versus tangential electric field for the normal electric fields of $4.0 \times 10^4, 9.0 \times 10^4, 1.3 \times 10^5$ and 3.0×10^5 V/cm, respectively. The solid line are the present simulation results and the broken lines are the drift velocities estimated from Cooper and Nelson's experimental formula. (a) simulation results using Model 1. (b) simulation results using Model 2. The threshold energies of $E_{th} = 0.09, 0.15, 0.16$ and 0.18 eV measured from the bottom of each inversion potential are taken respectively when the normal electric fields are $4.0 \times 10^4, 9.0 \times 10^4, 1.3 \times 10^5$ and 3.0×10^5 V/cm.

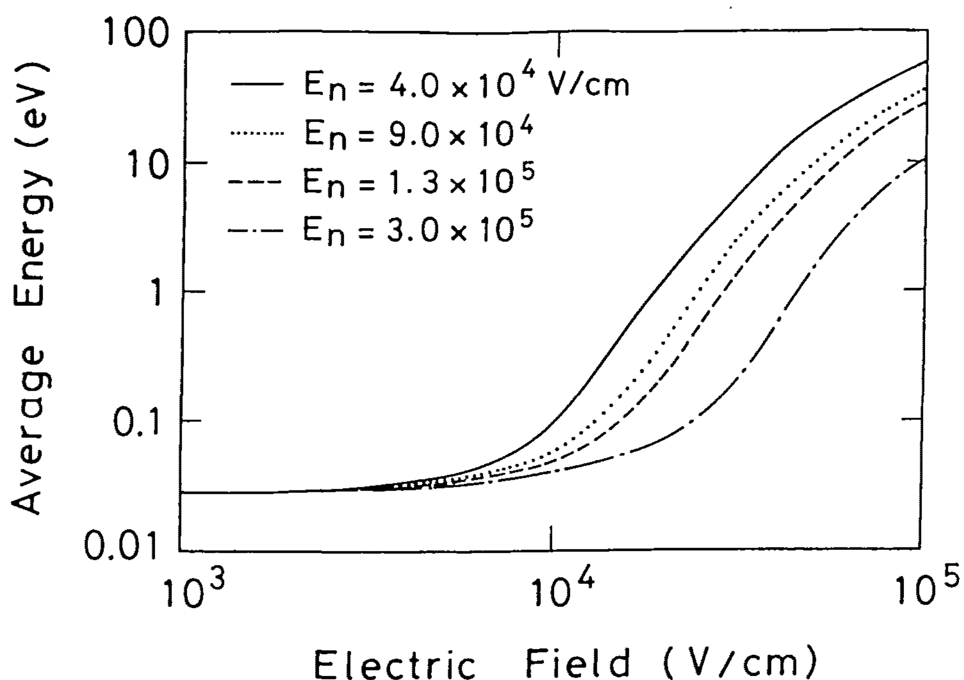

Figure 6: Averaged electron kinetic energy versus tangential electric field with the normal electric field as a parameter calculated using Model 1.

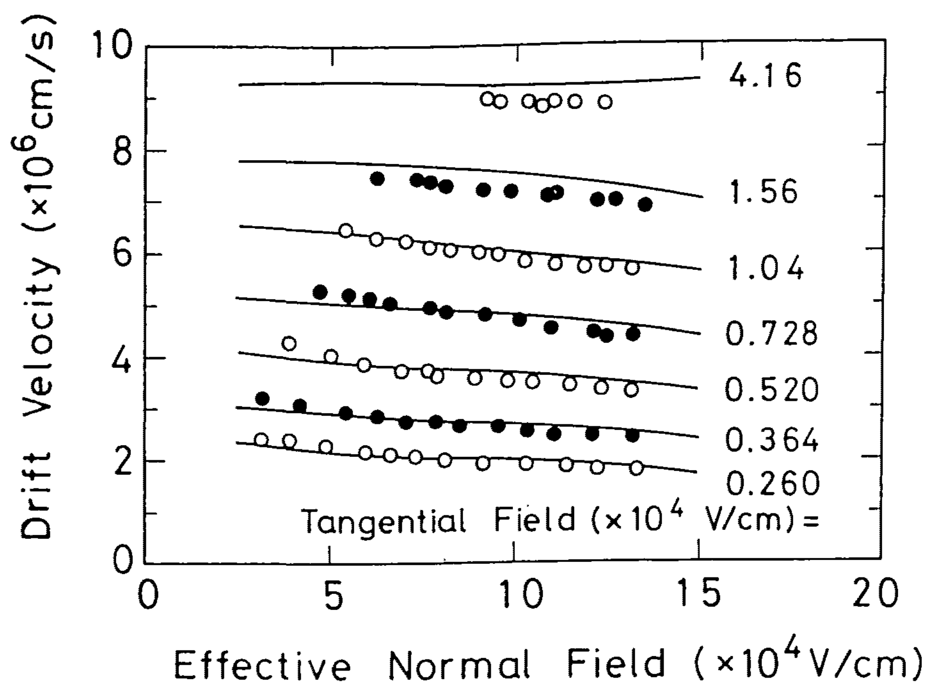

Figure 7: Comparison of the dependence of the drift velocity on the normal electric field with the tangential electric field as a parameter, using Cooper and Nelson's experimental results and the present sumulation using Model 2. The solid lines show the simulation results, and the dots and the circles are the experimental results of Cooper and Nelson.